

# Reduced Wafer-Scale Frequency Variation in Adiabatic Microring Resonators

Zhan Su,<sup>1,\*</sup> Ehsan S. Hosseini,<sup>1</sup> Erman Timurdogan,<sup>1</sup> Jie Sun,<sup>1</sup> Gerald Leake,<sup>2</sup> Douglas D. Coolbaugh,<sup>2</sup> and Michael R. Watts<sup>1</sup>

<sup>1</sup>Research Laboratory of Electronics, Massachusetts Institute of Technology, 77 Massachusetts Avenue, Cambridge, Massachusetts 02139, USA

<sup>2</sup>College of Nanoscale Science & Engineering, University at Albany, 1400 Washington Avenue, Albany, New York 12203, USA  
zhansu@mit.edu

**Abstract:** We experimentally demonstrate that adiabatic microring resonators not only achieve high quality factors in the presence of electrical contacts but, importantly, exhibit reduced susceptibility to wafer-scale fabrication induced resonant frequency variations compared to standard microrings.

**OCIS codes:** (130.0130) Integrated optics; (130.0250) Optoelectronics; (130.3120) Integrated optics devices.

## 1. Introduction

Microdisk resonators have been extensively used for applications requiring electrical or mechanical contact since interior contacts are naturally implemented [1]. However, microrings are generally preferred for high performance applications due to their large, uncorrupted free spectral ranges (FSR) that can, for example, accommodate more frequency channels on an optical communication line. Electrically or mechanically contacting these resonators without compromising their quality factors is essential for a number of applications such as electro-optic modulators [1-4], tunable filters [5-7], and optical sensors [8,9], which is, however, nontrivial considering the strong light-matter interaction in these resonant structures. To address this challenge, Watts recently proposed a new class of microring resonator, the adiabatic microring resonator [10], to provide low-loss, intimate electrical or mechanical contacts to the microring through an adiabatic structure, which has already been applied to modulators [3,4], tunable filters [6,7], and switches [7].

In this work, we optimize the geometry of adiabatic microring resonators using rigorous 3D finite-difference time-domain (FDTD) simulations, and experimentally demonstrate high-Q (7,000 for a 2- $\mu\text{m}$  radius and 27,000 for 3- $\mu\text{m}$  radius) adiabatic microring resonators in the presence of an electrical contact. The experimental results agree well with the numerical simulations. Importantly, wafer-scale measurements were performed to analyze the resonant wavelength variations of the adiabatic microring resonators across 54 dies in a 300-mm wafer fabricated with the advanced CMOS processing techniques. The statistical result shows that the wavelength uniformity of the optimized adiabatic microring resonator is twice as good as that of conventional microring resonators.

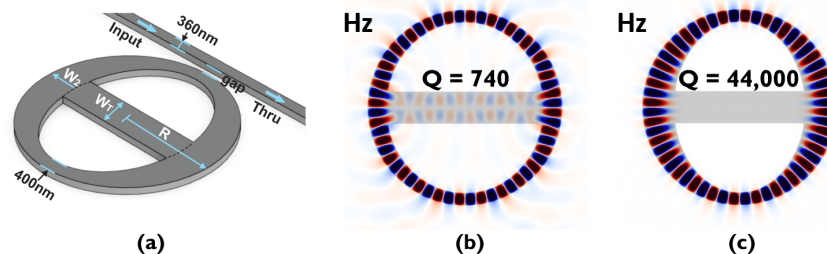


Fig. 1. (Color online) (a) Schematic of the adiabatic ring resonator. The bus waveguide width is 360 nm. The thickness of the structure is 220 nm. Properties such as the wider part of the AMR ( $W_2$ ) and tether width ( $W_T$ ) are marked. Mode profiles of 3- $\mu\text{m}$  radius adiabatic microring resonators with (b)  $W_2 = 0.6 \mu\text{m}$  and  $W_T = 1 \mu\text{m}$  and (c)  $W_2 = 1 \mu\text{m}$  and  $W_T = 1 \mu\text{m}$ .

Fig. 1(a) shows the schematic of the adiabatic microring resonator structure. Light is coupled from a 360-nm wide bus waveguide to the adiabatic microring resonator whose width gradually, or adiabatically, widens from 400 nm at the coupling point to  $W_2$  in a  $90^\circ$  bend. The adiabatic transition avoids the excitation of high-order modes so that an uncorrupted FSR can be achieved. The silicon contact with width  $W_T$  is introduced at the widest part of the adiabatic microring resonator where little optical field sees the silicon contact to avoid scattering loss. Fig. 1(b) and (c) show the simulated modes (Hz field) of adiabatic microring resonators with a narrower  $W_2$  (0.6  $\mu\text{m}$ ) and a wider  $W_2$  (1.0  $\mu\text{m}$ ) using 3D-FDTD in the presence of silicon contact. One can see that the optical mode in the one with

narrower contact region ( $W_2 = 0.6 \mu\text{m}$ ), which more resembles a conventional microring, suffers larger scattering loss than that in the optimized adiabatic microring resonator.

## 2. Measurement and Analysis

The adiabatic microring resonator structures were fabricated on a 300-mm silicon-on-insulator (SOI) wafer with 220 nm device layer, using 193-nm optical immersion lithography. Fig. 2(a) and (b) show the scanning-electron-micrographs (SEMs) images of the fabricated adiabatic microring resonators with 2- and 3- $\mu\text{m}$  radius. The corresponding transmission spectra around the resonance of the fabricated devices are shown in Fig. 2(c) and (d), showing clean FSRs and Qs as high as 7,000 for 2- $\mu\text{m}$  radius and 27,000 for 3- $\mu\text{m}$  radius.

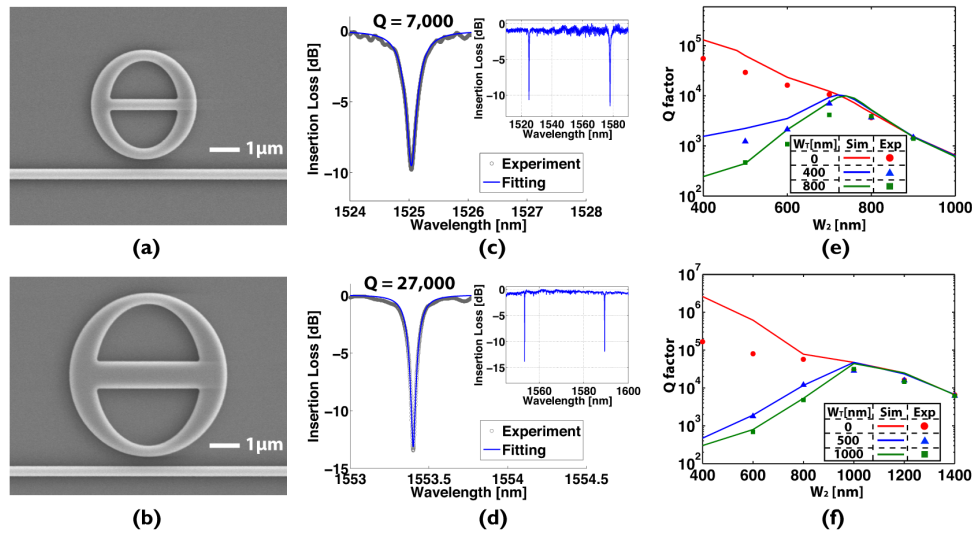


Fig. 2. (Color online) Top-view scanning-electron-microscope (SEM) images of the adiabatic microring resonator structure of (a) 2- $\mu\text{m}$  radius,  $W_2 = 0.7 \mu\text{m}$  and  $W_T = 0.4 \mu\text{m}$  and (b) 3- $\mu\text{m}$  radius,  $W_2 = 1 \mu\text{m}$  and  $W_T = 1 \mu\text{m}$ . Transmission spectrum of device of (c) 2- $\mu\text{m}$  radius and (d) 3- $\mu\text{m}$  radius. Insets are the spectra across one whole FSR. Intrinsic Q factors for (e) 2- $\mu\text{m}$  and (f) 3- $\mu\text{m}$  radius resonators with different  $W_2$  and  $W_T$  sizes.

A wide contact region ( $W_2$ ) avoids scattering loss from the silicon contact; however, if  $W_2$  is too large and the transition is too abrupt to be taken as adiabatic, high-order mode will be excited in the microring, causing excessive loss. Therefore, there exists an optimal waveguide width,  $W_2$ , at the point of contact that corresponds to the lowest loss. The quality factors of the adiabatic microring resonators at different waveguide widths  $W_2$ , were calculated using rigorous 3-D FDTD simulations, shown by the solid lines in Fig. 2(e) and (f). The highest Qs (9,950, 44,000) were achieved for waveguide widths  $W_2 = 740 \text{ nm}$  for a 2- $\mu\text{m}$  radius adiabatic microring resonator, and  $W_2 = 1000 \text{ nm}$  for the 3- $\mu\text{m}$  adiabatic microring resonator. To validate the simulation results, resonators with different waveguide widths  $W_2$ , contact widths  $W_T$ , and radiuses  $R$  were fabricated and measured to extract the quality factors, as shown by the dots in Fig. 2(e) and (f). The experiments agree well with the simulation; in particular, the optimized  $W_2$  sizes were accurately predicted by the simulation. High Qs (7,000, 27,000) were experimentally demonstrated in the 2- $\mu\text{m}$  and 3- $\mu\text{m}$  radius resonators in the presence of silicon contacts. Note that the experiments show much lower Qs compared to simulations in the resonators without contacts (red solid lines and dots in Fig. 2(e) and (f)) in the low loss region ( $Q > 1e5$ ), where the loss is dominated by the material absorption and surface roughness, which were not taken into account in the simulation.

Apart from high quality factor and a clean FSR, wafer-scale resonant wavelength uniformity is also essential for photonic resonators. The resonant wavelength variations of these resonators come from variations in Si thickness ( $T$ ), ring radius ( $R$ ) and width ( $W$ ). To separate the contribution of each component, microdisk resonators with 10- $\mu\text{m}$  designed radius, which have only thickness and radius variations, were first measured. The fabricated 300-mm wafer is shown in Fig. 3(a) with single reticle size of 32 mm by 26 mm. The standard deviations of resonant wavelengths (frequencies) of transverse electric (TE) and transverse magnetic (TM) inputs were measured to be 1.97 nm (246GHz) and 4.37 nm (545GHz) respectively. By analyzing the relation between TE and TM resonance shifts [11], the standard deviations of thickness and radius of the disk resonators were calculated to be 1.351 nm ( $\sigma_T$ ) and 3.735 nm ( $\sigma_R$ ). With the thickness and radius variations retrieved from microdisk measurements, microring structures were then measured across the wafer to find the width variation induced by lithographical imperfections.

Assuming independent distributions of thickness, radius and width, the standard deviation of resonant wavelength  $\lambda$  is then given by

$$\sigma(\lambda) = \sqrt{\left(\frac{\partial\lambda}{\partial T}\sigma_T\right)^2 + \left(\frac{\partial\lambda}{\partial R}\sigma_R\right)^2 + \left(\frac{\partial\lambda}{\partial W}\sigma_W\right)^2} \quad (1)$$

For a 3- $\mu\text{m}$  radius ring with width of 400 nm and height of 220 nm, the resonant wavelength change due to thickness, radius and width variations are 1.367 nm/nm ( $\partial\lambda/\partial T$ ), 0.291 nm/nm ( $\partial\lambda/\partial R$ ) and 0.894 nm/nm ( $\partial\lambda/\partial W$ ) respectively. The standard deviation of resonant wavelengths (frequencies) of conventional microring resonators is measured to be 5.38 nm (671GHz) (shown in Fig. 3(d)). According to Eq. (1), the width variation  $\sigma_W$  is 5.520 nm, outweighing the effects of other two degrees of freedom.

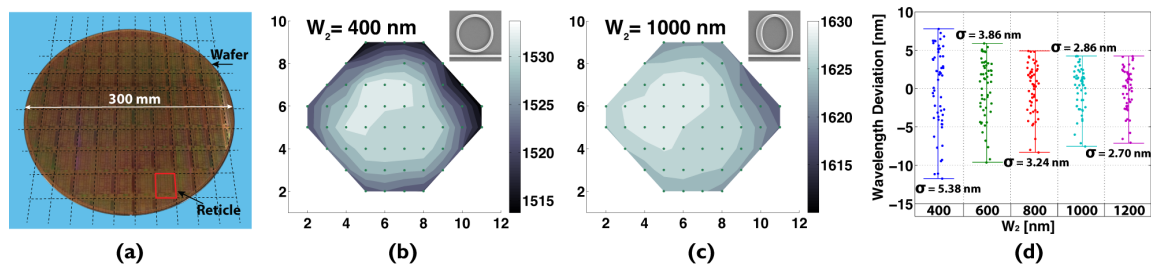


Fig. 3. (a) Fabricated 300-mm wafer with single reticle marked with red rectangle. Wavelength distribution across the wafer for (b)  $W_2 = 400$  nm and (c)  $W_2 = 1000$  nm. The dots represent the position of the measured chips. Insets are the SEMs of the corresponding adiabatic microring resonators. (d) Resonant wavelength variations across the wafer for various  $W_2$  sizes.

Resonant wavelengths of adiabatic microring resonators with different  $W_2$  sizes were then measured in 54 dies across the 300-mm wafer. Two examples ( $W_2 = 400$  nm and 1000 nm) of the resonant wavelength distributions are shown in Fig. 3(b) and (c). It is seen that the resonant wavelength distributions become more uniform with larger  $W_2$  sizes. The results are summarized in Fig. 3(d), showing a factor of two improvement in resonant wavelength uniformity by increasing  $W_2$  from 400 nm to 1200 nm. This improved fabrication tolerance is essential to wafer scale production of microring-based photonic structures such as multiplexers/demultiplexers for wavelength division multiplexing, optoelectronics modulators, etc.

### 3. Conclusions

Adiabatic microring resonators have been designed and demonstrated, revealing high quality factors, an uncorrupted FSR, and importantly, a reduced susceptibility to wafer-scale fabrication induced resonant frequency deviations. The combination of enhanced resonant frequency uniformity and the ability to contact adiabatic microring resonators for tuning and/or modulation without affecting the FSR, provide substantial reasons to consider the use of adiabatic microring resonators as a replacement for standard microring-resonators in nearly all communication applications.

This work was supported in part by the Defense Advanced Research Projects Agency (DARPA) Microsystems Technology Office's (MTO) E-PHI program, grant no. HR0011-12-2-0007.

### 4. References

- [1] M. R. Watts, W. A. Zortman, D. C. Trotter, R. W. Young, and A. L. Lentine, "Vertical junction silicon microdisk modulators and switches," *Opt. Express* **19**, 21989-22003 (2011).
- [2] Q. Xu, B. Schmidt, S. Pradhan, and M. Lipson, "Micrometre-scale silicon electro-optic modulator," *Nature* **435**, 325-327 (2005).
- [3] A. Biberman, E. Timurdogan, M. R. Watts, W. A. Zortman, and D. C. Trotter, "Adiabatic microring modulators," *Opt. Express* **20**, 29223-29236 (2012).
- [4] E. Timurdogan, C. M. Sorace-Agaskar, G. Leake, D. D. Coolbaugh, and M. R. Watts, "Adiabatic Resonant Microring (ARM) Modulators with Integrated Thermal Tuner," in *Advanced Photonics*, 2013, paper IT5A.7.
- [5] E. Timurdogan, E. S. Hosseini, G. Leake, D. D. Coolbaugh, and M. R. Watts, "L-Shaped Resonant Microring (LRM) Filter with Integrated Thermal Tuner," in *CLEO*, 2013, paper CTh4F.2.
- [6] M. Moresco, E. S. Hosseini, E. Timurdogan, D. D. Coolbaugh, G. Leake, and M. R. Watts, "Parallel-Coupled Adiabatic Resonant Microring (ARM) Filter with Integrated Heaters," in *CLEO*, 2013, paper CTh1C.5.
- [7] M. R. Watts, W. A. Zortman, D. C. Trotter, G. N. Nielson, D. L. Luck, and R. W. Young, "Adiabatic Resonant Microrings (ARMs) with Directly Integrated Thermal Microphotonics," in *Conference on Lasers and Electro-Optics/International Quantum Electronics Conference*, 2009, paper CPDB10.
- [8] M. R. Watts, M. J. Shaw, and G. N. Nielson, "Optical resonators: Microphotonic thermal imaging," *Nature Photon.* **1**, 632-634 (2007).
- [9] C. T. DeRose, M. R. Watts, D. C. Trotter, D. L. Luck, G. N. Nielson, and R. W. Young, "Silicon microring modulator with integrated heater and temperature sensor for thermal control," in *Conference on Lasers and Electro-Optics*, 2010, paper CThJ3.
- [10] M. R. Watts, "Adiabatic microring resonators," *Opt. Lett.* **35**, 3231-3233 (2010).
- [11] W. A. Zortman, D. C. Trotter, and M. R. Watts, "Silicon photonics manufacturing," *Opt. Express* **18**, 23598-23607 (2010).